Heating mechanisms for electron swarms in radio-frequency electric and magnetic fields

2015 Plasma Sources Sci. Technol. 24 054006

(http://iopscience.iop.org/0963-0252/24/5/054006)

IOP Publishing Plasma Sources Science and Technology

Plasma Sources Sci. Technol. **24** (2015) 054006 (13pp) doi:10.1088/0963-0252/24/5/054006

Heating mechanisms for electron swarms in radio-frequency electric and magnetic fields

S Dujko[1], D Bošnjaković[1], R D White[2] and Z Lj Petrović[1]

[1] Institute of Physics, University of Belgrade, Pregrevica 118, 11070 Belgrade, Serbia
[2] College of Science, Technology Engineering, James Cook University, Townsville 4810, Australia

E-mail: sasa.dujko@ipb.ac.rs

Received 27 March 2015, revised 29 June 2015
Accepted for publication 14 August 2015
Published 23 September 2015

Abstract

Starting from analytical and numerical solutions of the equation for collisionless motion of a single electron in time-varying electric and magnetic fields, we investigate the possible mechanisms for power absorption of electron swarms in neutral gases. A multi term theory for solving the Boltzmann equation is used to investigate the power absorption of electrons in radio-frequency (rf) electric and magnetic fields in collision-dominated regime for Reid's inelastic ramp model gas and molecular oxygen. It is found that the effect of resonant absorption of energy in oscillating rf electric and magnetic fields observed under conditions when collisions do not occur, carries directly over to the case where collisions control the swarm behavior. In particular, we have observed the periodic structures in the absorbed power versus amplitude of the applied rf magnetic field curve which have a physical origin similar to the oscillatory phenomena observed for collisionless electron motion. The variation of the absorbed power and other transport properties with the field frequency and field amplitudes in varying configurations of rf electric and magnetic fields is addressed using physical arguments.

Keywords: electron heating, Boltzmann equation, transport coefficients, electron swarms

(Some figures may appear in colour only in the online journal)

1. Introduction

Studies of electron swarms in neutral gases under the influence of varying configurations of electric and magnetic fields are of interest not only from a theoretical viewpoint but have many important applications such as determination of low-energy electron–molecule cross sections [1, 2], modeling of non-equilibrium plasma discharges, including magnetron sputtering [3, 4], plasma propulsion [5, 6] and inductively coupled plasma [7, 8], and modeling of particle detectors in high-energy physics [9, 10]. A swarm of charged particles is usually defined as an ensemble of charged particles, such as electrons or ions, drifting and diffusing in a background gas under the influence of electric and/or magnetic fields. In plasma physics, this is designated as the free diffusion or test particle limit where charged particle-charged particle interactions and space-charge fields are negligible. In plasma modeling, swarm data obtained under the influence of direct current (dc) electric (and rarely magnetic) fields are generally applied as input in fluid models of magnetized plasma discharges. In swarm experiments, the applied electric and magnetic fields as well as the properties of the background gaseous medium can be very efficiently controlled, enabling one to perform accurate measurements of transport coefficients. Transport coefficients can be then unfolded to yield information about cross sections for electron scattering which are required as input in kinetic models of plasma discharges. The literature of contemporary theoretical investigation on electron transport in electric and magnetic fields has been summarized in the papers of Petrović *et al* [2, 11], White *et al* [12, 13] and Dujko *et al* [14, 15], with particular emphasis on dc electric and magnetic fields.

For the more general case of alternatively current (ac) electric and magnetic fields, particularly in domain of rf fields crossed at arbitrary phases and angles, there has been comparatively less investigation. The reason is twofold: first, the presence of time-varying magnetic field introduces unavoidable mathematical complexity in theories for solving the Boltzmann equation and second, still it is not entirely clear how to implement time-resolved swarm transport data in fluid

models of magnetized plasma discharges properly. In addition, it is very computationally expensive to store space and time-dependent distribution functions and related transport data and usually the cycle-averaged values for these quantities are employed in the models [16]. Nevertheless, the existence of crossed rf electric and magnetic fields in inductively coupled plasmas, rf magnetrons and in some other types of magnetically enhanced plasma sources have triggered a new wave of studies of the equivalent swarm problem. One of the critical problems in these studies was accurate representation of temporal and spatial non-locality of electron transport in various field configurations [17–20]. Certain aspects of the same problem are addressed by plasma modelers without taking advantage of the recent advances in the physics of swarms. In particular, kinetic phenomena induced by temporal non-locality of electron transport in time-varying fields such as anomalous anisotropic diffusion [21, 22], time-resolved negative differential conductivity [23] and transiently negative diffusivity [24, 25], as well as phenomena induced by the explicit influence of non-conservative collisions such as the absolute negative electron mobility [26], are such examples. The influence of a time-varying magnetic field on electron kinetics was also rarely studied in plasma modeling with the exception of some Particle in Cell models [27–29]. A few authors have considered the $\mathbf{E} \times \mathbf{B}$ transport data into plasma models accurately which in turn have led to a better understanding of the plasma heating for some arrangements of magnetically enhanced/assisted plasma reactors [16, 30]. It was also shown that inclusion of the $\mathbf{E} \times \mathbf{B}$ drift may lead to additional heating of inductively coupled plasmas [31, 32]. Kinetic phenomena induced by temporal and spatial non-locality, their interpretation and physical implications which may arise from their explicit inclusion into plasma models, have given rise to a whole new dimension of swarm physics. The literature of theoretical investigation on electron swarms in rf electric and magnetic fields has been recently summarized in the papers [2, 11, 13, 33], textbook [7] and thesis [34].

In this paper, as a part of our on-going investigations of electron transport in spatially uniform rf electric and magnetic fields, we systematically study the origin and physical mechanisms for electron heating assuming swarm conditions. Preliminary results revealed the existence of periodic structures in the variation of the mean energy with the magnetic field amplitude for certain model gases [35]. This phenomenon was related to the resonant absorption of energy from rf fields by electrons. Similar results have never been observed for electrons in dc electric and magnetic fields, where the mean energy of electrons is always a monotonically decreasing function of magnetic field strength, independent of the gas type and field configuration (except for parallel fields) [12, 14, 15, 36–38] and with the exception of one observation of local peaks in energy for electron swarms in argon [39]. This raises a number of questions: Which physical mechanism controls the power absorption in rf electric and magnetic fields? What is the nature of the periodicity and spacing between individual peaks in the profile of the absorbed power? Does the phenomenon occur for real gases or only for less realistic model gases? What are the implications of this phenomenon for analysis of power absorption in more realistic plasma sources? In this paper we will try to address some of these issues. In particular, here we do not attempt to analyze the ohmic, and stochastic heating by anomalous skin effect [40–44], and related electrodynamics of electrons in realistic rf plasma sources where many parameters and operating conditions such as pressure, coil design [45, 46] and antenna shape [47], and presence of a substrate [48] as well as gas heating [49] may simultaneously affect the mechanisms for power absorption. Examples of these studies include those attempting to understand the non-local power deposition in inductively coupled plasmas [50–52], rf magnetrons [53] and magnetically enhanced plasmas. Instead we isolate and investigate the electron component of these plasmas under the action of spatially uniform rf electric and magnetic fields. We believe that one of the most critical steps in plasma modeling is testing and verification of plasma models and interpretations against swarm-type models and spatially uniform fields. In particular, due to their complexity and due to difficulties associated with the implementation of boundary conditions to solutions of Boltzmann's equation, kinetic treatments of non-equilibrium plasmas sustained by rf electric and magnetic fields should be benchmarked against the swarm results in the free diffusion limit. On the other hand, one ought to mention the recent study on the non-local response and resonance phenomena associated with electrons subjected to an externally prescribed, spatially varying electrostatic field [54].

This work represents the first multi term Boltzmann equation calculation of power absorption of the electrons in rf electric and magnetic fields under swarm conditions. The study is organized as follows. In section 2, we first consider the collisionless motion of a single electron in oscillating rf electric field, then we proceed to a combined rf electric and dc magnetic fields case, and finally we analyze the motion of a single electron in oscillating rf electric and magnetic fields. In this section, particular emphasis is placed upon the derivation of conditions for resonance. The explicit influence and contribution of collisions between electrons and neutral molecules to power absorption is examined via Boltzmann's equation analysis. In the same section we analyze the role of collisions on the power absorption by considering the electron transport in varying configurations of electric and magnetic fields. Our specific interest here is to investigate relations with the collision free case. Temporal profiles and cycle-averaged values of various transport properties are presented as a function of the field frequency and field amplitudes for Reid's inelastic ramp model and molecular oxygen. In section 4 we discuss the periodic resonant structures that exist in the profiles of the absorbed power and mean energy with magnetic field amplitude in rf electric and magnetic fields.

2. Collisionless motion of a single electron in uniform and time-varying electric and magnetic fields

In this section we are concerned with the collisionless motion of electrons in spatially uniform electric and magnetic fields perpendicular to each other. While some of the

issues discussed here may be well known, it is necessary to present them to build a phenomenology for the effect of the magnetic field in collisionless and collisional conditions. The assumption of motion without collisions is applicable when electron performs a large number of oscillations between two successive collisions. Let us assume that the electric field lies along the z-direction while magnetic field is oriented along the y-direction. The equations of collisionless electron motion are then given by:

$$m\frac{\mathrm{d}v_x}{\mathrm{d}t} = ev_zB(t), \tag{1}$$

$$m\frac{\mathrm{d}v_y}{\mathrm{d}t} = 0, \tag{2}$$

$$m\frac{\mathrm{d}v_z}{\mathrm{d}t} = -e(E(t) + v_xB(t)), \tag{3}$$

where e and m are the electron charge and mass. In what follows the subdivision is made by considering the following cases: (1) time-varying electric and no magnetic field, (2) time-varying electric field and static magnetic field, and (3) time-varying electric and time-varying magnetic fields. The detailed consideration of electron orbits in electric and magnetic fields is beyond the scope of this paper and our focus is placed upon the power absorption by electrons.

2.1. Interaction of electrons with a time-varying electric field

Let us consider now the interaction of electrons with a spatially uniform and time-varying electric field, $E = E_0 \cos \omega t$ in magnetic field free case. Solving equations (1)–(3), we obtain for the three velocity components

$$v_x = v_{x0}, \quad v_y = v_{y0}, \quad v_z = -\frac{eE_0}{m\omega}\sin \omega t + v_{z0}, \tag{4}$$

where v_{x0}, v_{y0} and v_{z0} are initial velocities. Integrating equation (4) we obtain for the displacement of the electron the components

$$x = v_{x0}t + x_0, \quad y = v_{y0}t + y_0, \quad z = \frac{eE_0}{m\omega^2}\cos \omega t + v_{z0}t + z_0, \tag{5}$$

where x_0, y_0 z_0 are initial positions.

From equations (4) and (5) we see that an electron oscillates at the frequency of the field. The displacement is in phase with the field while the velocity is out of phase by $\pi/2$. Thus if collisions do not occur, then the electric field on the average does no work, on an electron. Using the vector notation, equations (4) and (5) imply that

$$\langle -e\mathbf{E}\cdot\mathbf{v}\rangle = \frac{-eE_0^2}{m\omega}\langle \cos \omega t \sin \omega t\rangle - e\mathbf{E}_0\cdot\mathbf{v}_0\langle \sin \omega t\rangle = 0\ , \tag{6}$$

where angle brackets denote time averaging. Therefore, for collisionless electron motion the energy gained during one half of the field cycle is returned to the field in the other half of the cycle, and no energy can be transferred.

For power absorption to occur there must be some randomization mechanisms that break the regularity and coherence of the electron motion and the $\pi/2$ phase shift between the velocity and electric field. As it is well known, phase mixing required for electrons to achieve net mean energy is due to collisions with the neutral background gas. Collisions between the electrons and neutral molecules perturb the phase, thereby disturbing the purely harmonic course of the electron's oscillations. Alternatively, reflection from a moving field gradient which is common in rf plasmas will also lead to heating even without collisions [8].

The time-averaged power absorbed by the swarm (or plasma or any active medium), p_{abs}, is given by

$$\langle p_{\mathrm{abs}}\rangle = \frac{1}{T}\int_0^T -eN\mathbf{W}(t)\cdot\mathbf{E}(t)\,\mathrm{d}t\ , \tag{7}$$

where N is the number of electrons in the swarm, $T = 2\pi/\omega$ is the period, and $\mathbf{W}(t)$ is the average velocity. It should be noted that the number of electrons N is not generally conserved due to number changing processes such as electron attachment or ionization. From equation (7) we see that in the time intervals when the drift velocity (or current for plasmas) and electric field have the same sign, the instantaneous power is positive and the electric field pumps energy into the system. Conversely, when the drift velocity and electric field have the opposite signs the instantaneously power is negative and the energy is transfered from an active medium to the external circuit. This suggests that a phase difference between the drift velocity and electric field controls the power absorption of the electrons. This is illustrated schematically in figure 1.

2.2. Interaction of electrons with a time-varying electric field and static magnetic field

In this section we analyze the collisionless motion of electrons in time-varying electric $E = E_0 \cos \omega t$ and static magnetic fields. Solving equations (1)–(3), we obtain for the Cartesian components of the velocity

$$v_x(t) = v_{x0}\cos \Omega t + v_{z0}\sin \Omega t + \frac{e}{m}\frac{E_0\Omega}{\Omega^2-\omega^2}(\cos \Omega t - \cos \omega t), \tag{8}$$

$$v_y(t) = v_{y0}, \tag{9}$$

$$v_z(t) = v_{z0}\cos \Omega t - v_{x0}\sin \Omega t - \frac{e}{m}\frac{E_0}{\Omega^2-\omega^2}(\Omega \sin \Omega t - \omega \sin \omega t), \tag{10}$$

where v_{x0}, v_{y0} and v_{z0} are initial velocities and $\Omega = eB/m$ is the cyclotron frequency of gyration of the electrons about the magnetic field lines. Integrating equations (8)–(10) the displacement components of the electron can be derived. In brief, magnetic field rotates electrons which have elliptical orbits in $(\mathbf{E}, \mathbf{E}\times\mathbf{B})$ plane (e.g. in x–z plane) and the motion of electrons has components at both the cyclotron frequency and at the frequency of the electric field ω. The major characteristics

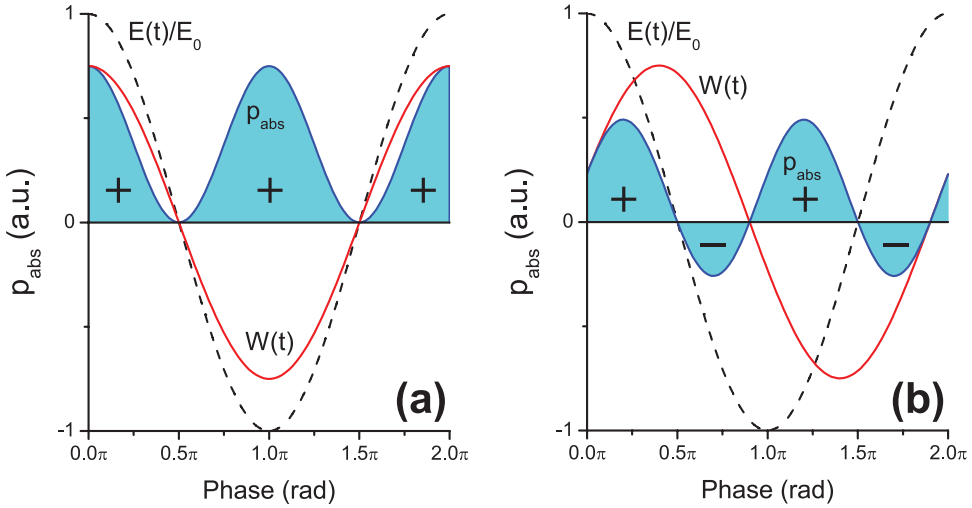

Figure 1. Schematic diagrams of power absorption for charged particle swarms when there is only electric field: (a) no phase difference between the drift velocity and electric field; (b) the phase difference of $2\pi/5$ between the drift velocity and electric field.

of the orbits are dependent on the ratio Ω/ω. In particular for the singular case $\Omega = \omega$, the electron moves in circles of ever increasing radii. This is the well-known cyclotron resonance effect. During this spiral motion the velocity of electron continually increases. Since its kinetic energy increases the electron absorbs energy from the time-varying rf field. This absorption of energy is a resonant process but as we will see later the singular case $\Omega = \omega$ does not correspond to the maximum absorption of energy.

The instantaneous absorbed power for an arbitrary instant of time is given by

$$p_{\mathrm{abs}}(t) = -ev_z(t)E_0 \cos \omega t, \tag{11}$$

while for the time-averaged power absorbed by an electron, we find

$$\langle p_{\mathrm{abs}} \rangle = \frac{1}{T}\int_0^T p_{\mathrm{abs}}(t)\,\mathrm{d}t = \frac{2}{m}\left(\frac{eE_0\Omega \sin\frac{\pi\Omega}{\omega}}{\Omega^2-\omega^2}\right)^2. \tag{12}$$

Assuming the field frequency of 500 MHz and an electric field amplitude of 200 Td (1 Td $= 1 \times 10^{-21}$ Vm^2), in figure 2 we display the time-averaged power as a function of the reduced magnetic field strength (1 Hx $= 1 \times 10^{-27}$ Tm^3). In order to facilitate comparisons with the collisional case we shall use E/n_0 and B/n_0 values in both cases to label conditions. Having in mind that when $n_0 = 0$ the ratio E/n_0 and/or B/n_0 is meaningless in collisionless case, it should, however, represent the same field. For example, when $E/n_0 = 200$ Td the electric field is actually 7080 V m^{-1} and when $B/n_0 = 570$ Hx the magnetic field is 20.2 mT. It should be noted that selected values for frequency and field strengths used to calculate the absorbed power, correspond to those used in section 3.4 where collisions occur and where the power absorption is studied for electrons in molecular oxygen.

The resonant and periodic features in the profile of $\langle p_{\mathrm{abs}} \rangle$ with B/n_0 shown in figure 2 are clearly evident. According to equation (12) the positions of minima (or anti-resonances) where the absorbed power is zero, are simply given by

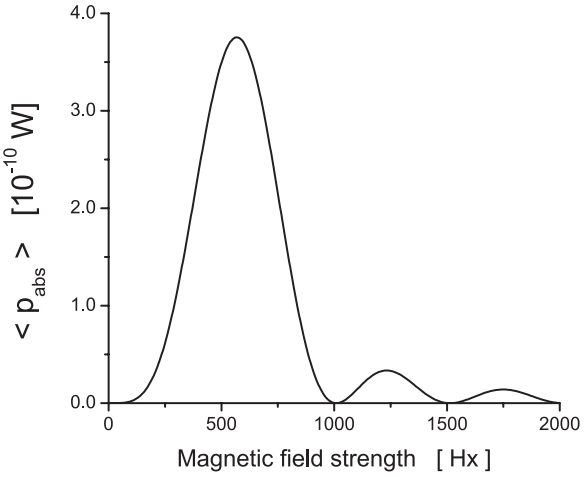

Figure 2. Variation of the time-averaged power for collisionless motion of a single electron with dc magnetic field strength. The amplitude of electric field is 200 Td (which corresponds to 7080 V m^{-1}).

$$\Omega = k\,\omega, \qquad (k \in \mathbf{N_0} \setminus \{1\}), \tag{13}$$

where $(k \in \mathbf{N_0} \setminus \{1\})$ indicates all natural numbers including 0 but without 1. This suggests that the spacing in the magnetic fields between two successive minima corresponds to the field frequency.

For positions of peaks we find

$$\frac{\Omega}{\omega} = \frac{1}{\pi}\mathrm{arccot}\left[\frac{\omega(\Omega^2+\omega^2)}{\pi\Omega(\Omega^2-\omega^2)}\right] + m, \qquad (m \in \mathbf{N}), \tag{14}$$

where m is any natural number. Equation (14) is transcendent and reflect the periodicity of the peak occurrence. It should be noted that the spacing between two successive peaks generally is not constant due to the first term in equation (14). However, if Ω dominates ω the first term approaches to 1/2 and spacing between two successive peaks now becomes constant. Note that according to equations (13) and (14) the positions of the extremes are determined exclusively by the ratio

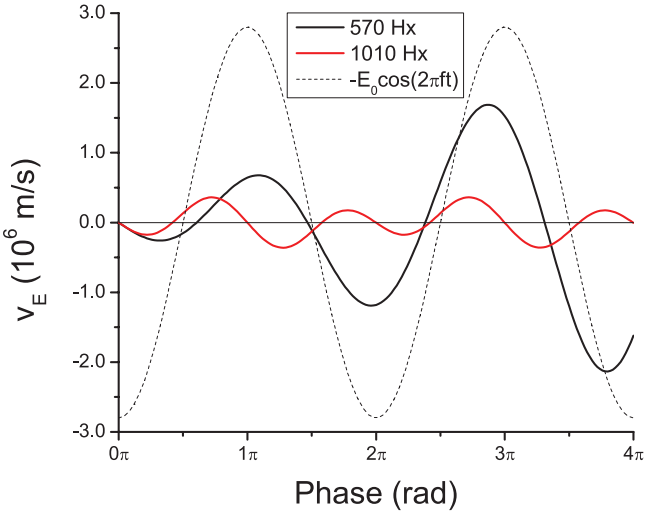

Figure 3. Temporal profiles of the longitudinal velocity for collisionless motion of a single electron in time-varying electric and dc magnetic fields. The amplitude and frequency of the electric field are 200 Td (7080 V m^{-1}) and 500 MHz while magnetic field strengths are 570 (20.2 mT) and 1010 Hx (35.8 mT).

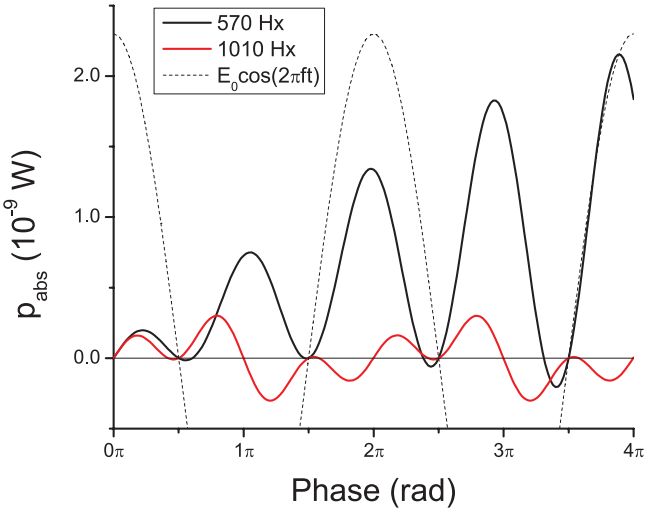

Figure 4. Temporal profiles of the instantaneous power for collisionless motion of a single electron in time-varying electric and dc magnetic fields. The amplitude and frequency of the electric field are 200 Td (7080 V m^{-1}) and 500 MHz while magnetic field strengths are 570 Hx (20.2 mT) and 1010 Hx (35.8 mT).

Ω/ω. Moreover, it is interesting to note that for a selected set of initial conditions used to evaluate the power, positions of extremes in variation of $\langle p_{\rm abs} \rangle$ with B/n_0 are not related to the singular case of cyclotron resonance $\Omega = \omega$.

In figure 3 we show temporal profiles of the longitudinal ($v_E = v_z$) velocity components for magnetic field strengths of 570 and 1010 Hx, respectively. Calculations are performed for the first two periods of the electric field. The values of B/n_0 of 570 and 1010 Hx are deliberately chosen as the first peak and first minimum in the absorbed power versus amplitude of the applied magnetic field curve correspond to these values (see figure 2). For B/n_0 of 1010 Hx, the longitudinal velocity is perfectly periodic, its amplitude stays unaltered and its mean value is zero. Conversely, for B/n_0 of 570 Hx, longitudinal velocity is not periodic, its amplitude continuously increases with time and its mean value is non-zero. This suggests that an electron continuously absorbs the energy from the fields which is demonstrated in figure 4 where the temporal profile of the instantaneous power is shown. In contrast to the $B/n_0 = 570$ Hx case, for B/n_0 which corresponds to the first minimum in the B/n_0 profile of $\langle p_{\rm abs} \rangle$ (e.g. for 1010 Hx), we see that the mean value of the instantaneous power is zero.

2.3. Interaction of electrons with time-varying electric and time-varying magnetic fields

We now consider the case of time-varying electric and time-varying magnetic fields. The solution of equations (1)–(3) cannot be obtained in a closed-form. Instead, we apply a numerical method described by Dormand and Prince [55] which is based on Runge–Kutta formulas. Various implementations of this method are publicly available. In order to demonstrate the effect of time-varying magnetic fields, equations (1)–(3) are numerically solved assuming $E/n_0 = 200$ Td, $f = 500$ MHz and a range of magnetic field amplitudes B_0/n_0. The same electric field amplitude and field frequency will be applied in section 3.5 where the power absorption is studied for electrons in molecular oxygen under conditions in which the swarm behavior is controlled by collisions.

The solutions calculated using the initial values $v_{x0} = v_{z0} = 0$ are shown in figures 6 and 7. We observe that the mean absorbed power during the first period of the rf field exhibits a strong resonant behavior (figure 5) but the conditions for resonance are not the same as in the case of a static magnetic field. These conditions are discussed in more detail in section 4. The longitudinal velocity (see figure 6) and the instantaneous absorbed power (see figure 7) are calculated using two different magnetic field amplitudes, 950 Hx and 1950 Hx, which correspond to the resonance and anti-resonance, respectively. It is seen that in the case of resonance, the amplitude of the longitudinal velocity (v_E) increases with time and so does the absorbed power. In case of anti-resonance, the energy absorbed during one period is almost zero and the velocity components are periodic functions with essentially constant amplitudes.

3. Motion of electrons in uniform and time-varying electric and magnetic fields in the presence of collisions

3.1. Brief description of theoretical methods

The heating mechanism for electron swarms in the presence of collisions under the action of rf electric and magnetic fields is investigated using a multi term theory for solving the Boltzmann equation. A detail discussion of the Boltzmann equation based calculation used in this work to evaluate power and various electron transport parameters may be found elsewhere [17, 33, 36]. A Monte Carlo simulation technique is also used in this work but as an independent tool with the aim of verifying the sometimes atypical

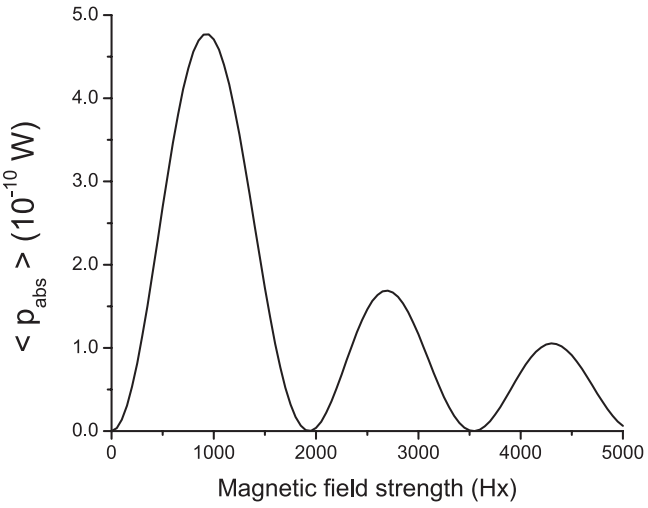

Figure 5. Variation of the time-averaged power for collisionless motion of a single electron with the amplitude of rf magnetic field. The amplitude of the electric field is 200 Td (7080 V m^{-1}) and frequency is set to 500 MHz.

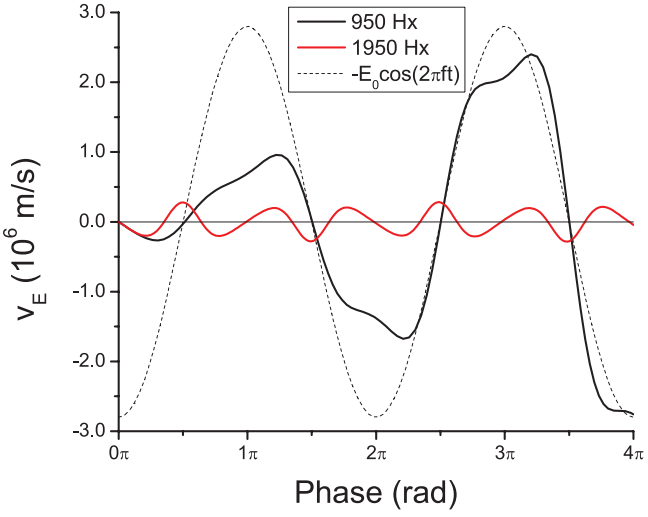

Figure 6. Temporal profiles of the longitudinal velocity for collisionless motion of a single electron in time-varying electric and magnetic fields. The amplitude and frequency of the fields are 200 Td (7080 V m^{-1}) and 500 MHz while magnetic field amplitudes are 950 Hx (33.6 mT) and 1950 Hx (69 mT).

behavior of electron transport properties in rf electric and magnetic fields found in the Boltzmann equation solutions. Some examples of atypical behavior include the negative diffusion coefficients, asymmetry of the drift velocity along the $\mathbf{E}\times\mathbf{B}$ direction with respect to zero value or the presence of additional oscillatory type-behavior in the temporal profiles of drift velocity components and in the profiles of individual diffusion tensor elements. In addition, we use our Monte Carlo method to follow the spatio-temporal development of an electron swarm in the real space which can be very useful to understand the behavior of electron transport properties in rf electric and magnetic fields, particularly if electron transport is greatly affected by non-conservative collisions. For more details on our Monte Carlo technique the reader is referred to [11, 56, 57].

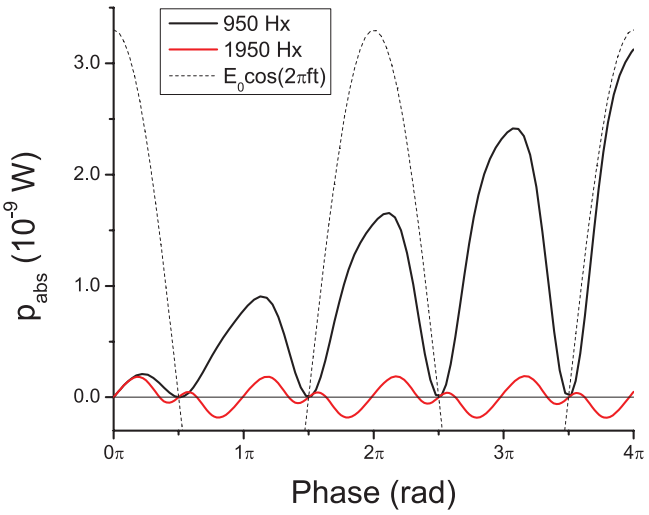

Figure 7. Temporal profiles of the instantaneous power for collisionless motion of a single electron in time-varying electric and magnetic fields. The amplitude and frequency of the electric field are 200 Td (7080 V m^{-1}) and 500 MHz while magnetic field amplitudes are 950 Hx (33.6 mT) and 1950 Hx (69 mT).

3.2. Preliminaries

In order to illustrate the power absorption of electrons in rf electric and magnetic fields under swarm conditions, we first consider Reid's inelastic ramp model [59]. This model has been used many times in the past to test various theories for solving Boltzmann's equation and numerical accuracy of different Monte Carlo codes for electron transport. Various conditions have been considered, including dc electric and magnetic fields [12, 37, 38, 60], as well as time-varying electric and magnetic fields [11, 17, 25, 61] for a variety of field configurations. The details of the model used here are as follows:

$$\begin{aligned}
&\sigma_m(\epsilon) = 6\,\mathring{A}^2 \quad \text{(elastic cross section)}\\
&\sigma_{inel}(\epsilon) = \begin{cases} 10(\epsilon-0.2)\,\mathring{A}^2, & \epsilon \geqslant 0.2\ \text{eV} \\ 0, & \epsilon < 0.2\ \text{eV} \end{cases} \quad \text{(inelastic cross section)}\\
&m_0 = 4\ \text{amu}\\
&T_0 = 0\text{K}\,,
\end{aligned} \tag{15}$$

where m_0 and T_0 represent the mass and temperature of the neutral gas particles while ϵ has the units of eV.

The failure of the classical two term approximation for solving Boltzmann's equation for Reid's inelastic ramp model is well-documented [37, 58, 59] and generally $l_{\max} = 4$ is required to achieve convergence of transport coefficients to within 0.5%. On the other hand, as pointed out by White *et al* [66] and Dujko *et al* [17], the application of a magnetic field acts to destroy the anisotropy of the velocity distribution function, consequently inducing enhanced convergence in the l-index. Nevertheless, all calculations are performed assuming $l_{\max} = 4$.

In addition to Reid's inelastic ramp model, we investigate the power absorption of the electrons in molecular oxygen. The cross sections for electron scattering in molecular

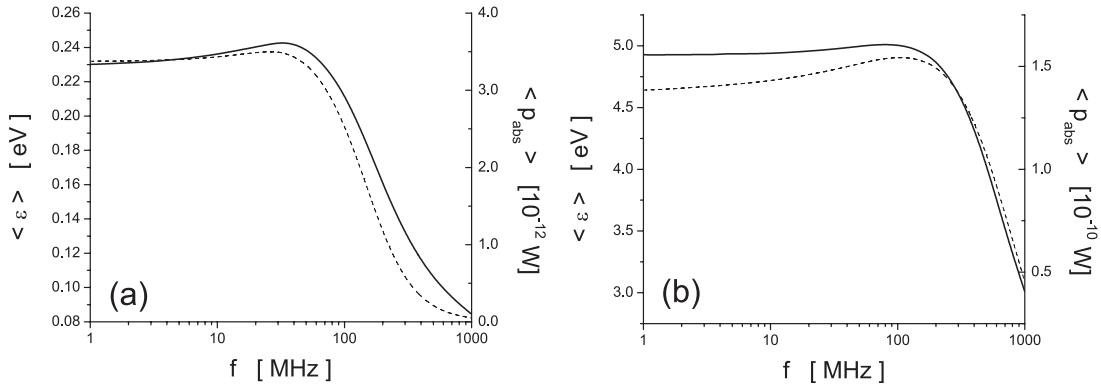

Figure 8. Variation of the cycle-averaged mean energy (full line) and power (dash line) with the frequency of the applied rf electric field. Calculations are performed for (a) Reid's inelastic ramp model ($E_0/n_0 = 14.14$ Td) and (b) molecular oxygen ($E_0/n_0 = 200$ Td).

oxygen are detailed in [62, 63] and displayed in [17]. The same set of cross sections was successfully applied for determination of the steady-state electron transport coefficients and for the studies of the temporal relaxation of electrons when electric and magnetic fields are crossed at arbitrary angles [17, 64]. Calculations are performed for low pressures ($p \leqslant 1$ Torr) and while the effects of three-body attachment are included in this study, these effects are negligible in the limit of low pressures, as discussed in [65]. The two-term approximation for solving Boltzmann's equation for electrons in molecular oxygen fails due to large cross sections for inelastic collisions and due to their rapid rise with the electron energy. As for Reid's inelastic ramp model, it was found that a value of $l_{\max} = 4$ is required to achieve the convergence to within 1% for the transport properties of interest in the present work.

All calculations are performed for zero gas temperature and the neutral gas number density is fixed to 3.54×10^{22} m^{-3}. The electric field has the following form $E(t)/n_0 = (E_0/n_0)\cos(2\pi ft)$ Td while magnetic field is treated differently. In section 3.3 we consider magnetic field free case while in section 3.4 we consider rf electric and dc magnetic fields. In section 3.5 the electric and magnetic fields are radio-frequency. In particular, if electric and magnetic fields are $\pi/2$ out of phase then magnetic field has the following form $B(t)/n_0 = (B_0/n_0)\sin(2\pi ft)$ Hx, where B_0/n_0 is magnetic field amplitude. All calculations deal exclusively with the $\mathbf{E} \times \mathbf{B}$ configuration.

3.3. Electrons in a time-varying rf electric field in the presence of collisions

In figures 8(a) and (b) we show the cycle-averaged mean energy $\langle\varepsilon\rangle$ and cycle-averaged power $\langle p_{\text{abs}}\rangle$ as a function of the frequency of the applied rf electric field for Reid's inelastic ramp model and molecular oxygen, respectively. For both gases the cycle-averaged value of mean energy and the cycle-averaged value of power display a maximal property with frequency. We see that both $\langle\varepsilon\rangle$ and $\langle p_{\text{abs}}\rangle$ decrease rapidly for higher frequencies. For Reid's inelastic ramp model the maximum in $\langle\varepsilon\rangle$ occurs at approximately 35 MHz while for $\langle p_{\text{abs}}\rangle$ the maximum is at approximately 27 MHz. For oxygen, the maximum in $\langle\varepsilon\rangle$ occurs at higher frequencies, around 100 MHz while $\langle p_{\text{abs}}\rangle$ attains its maximal value around 80 MHz. The instantaneous power relaxes on the time scale of momentum relaxation while the mean energy relaxes according to the time constant for energy transfer in collisions. As discussed by Dujko *et al* [17], for molecular oxygen the relaxation of momentum is a much faster process. As a consequence, the mean energy undergoes a reduction in modulation amplitude and exhibits a phase shift with respect to the electric field in the range of field frequencies for which the drift velocity is almost fully modulated.

Temporal profiles of the mean energy ϵ and drift velocity W as a function of the frequency of the applied rf electric field for electrons in oxygen are shown in figure 9. These profiles are used to evaluate the cycle-averaged values shown in figure 8. For ϵ we note the following: (1) the modulation amplitude decreases with increasing frequency and is essentially time-independent in the limit of the highest frequencies considered in this work; (2) the phase delay of the temporal energy profile with respect to the applied electric field increases with increasing frequency; (3) as already discussed ϵ exhibits a maximal property with frequency; and (4) there is a transition from non-sinusoidal profiles at low frequencies to sinusoidal at higher frequency.

From the profiles of the drift velocity W we note the following: (1) the modulation amplitude shows a maximal property with the field frequency; (2) there are no signs of time-resolved negative differential conductivity; and (3) there is transition from non-sinusoidal profiles at lower frequencies to sinusoidal at higher frequency.

Among the many important points which can be observed in the temporal profiles displayed in figures 9(a) and (b), it is clear that due to collisions between electrons and neutral background molecules the coherence of the electron motion and the $\pi/2$ phase shift between the velocity and electric field is broken. For swarms under the influence of an rf electric field in low-frequency regime, the effective relaxation times for momentum and energy are sufficiently small over all phases of the field, that full relaxation applies and drift velocity follows the field in a quasi-stationary manner. In such a case, the time-averaged power absorbed by the swarm

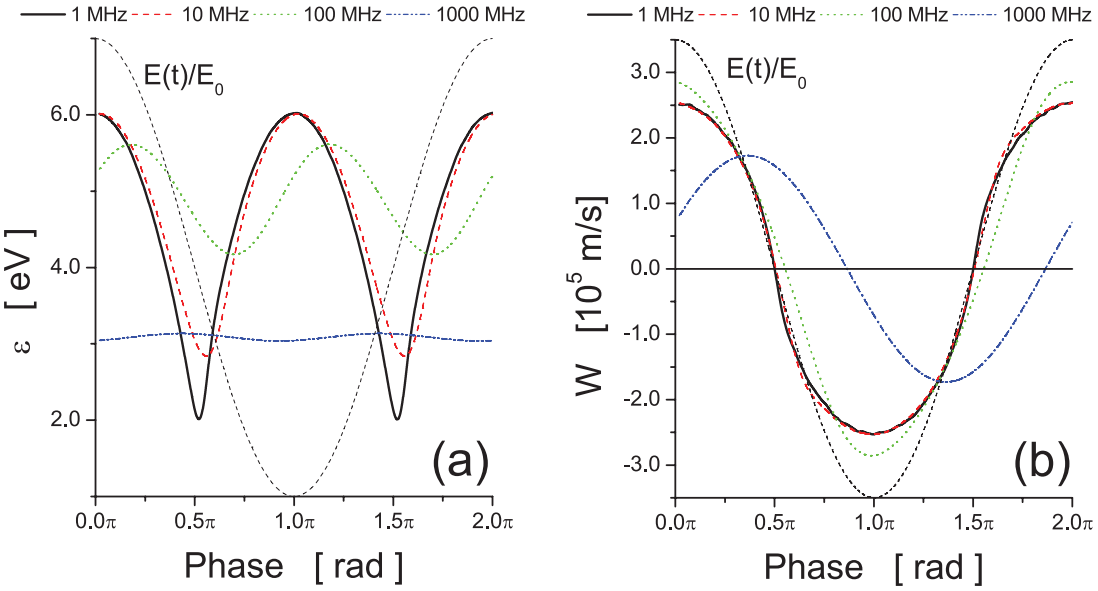

Figure 9. Temporal profiles of the mean energy (a) and drift velocity (b) as a function of the frequency of the applied rf electric field. The amplitude of electric field is 200 Td and calculations are performed for molecular oxygen.

depends on the magnitude of the drift velocity and shape of the drift velocity temporal profile. As proposed by Bzenić *et al* [23], the time-resolved negative differential conductivity in the temporal profiles of the drift velocity can enhance/reduce the overlap between the drift velocity and electric field. As a consequence, the power absorption by the swarm could be increased/reduced. On the other hand, for an increasing field frequency the phase difference between the drift velocity and electric field is increased due to the inability of both momentum and energy to sufficiently relax before the field changes. As a consequence, the drift velocity undergoes a reduction in the modulation and an increase in the phase shift with respect to the field which in turn leads to reduction of the power absorption. It should be noted that various effective field theories for electron transport in rf electric fields such as quasi-stationary or effective field approximations usually fail to accurately describe the power absorption [11, 23].

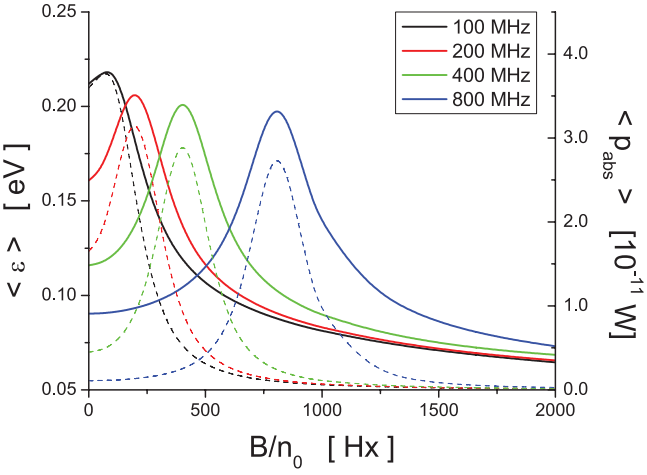

Figure 10. Variation of the cycle-averaged mean energy (full lines) and cycle-averaged absorbed power (dash lines) with B/n_0 for different field frequencies f. Calculations are performed for Reid's inelastic ramp model. The amplitude of electric field is 14.14 Td.

3.4. Electrons in a time-varying rf electric field and static magnetic field in the presence of collisions

In this section we analyze the power absorption of the electrons in time-varying rf electric and static magnetic fields in the presence of collisions. Figures 10 and 11 display the variation of the cycle-averaged mean energy and cycle-averaged power as a function of the applied magnetic field strengths for Reid's inelastic ramp model and molecular oxygen, respectively. We observe that the positions of peaks in the $\langle\varepsilon\rangle$ approximately correspond to those of the $\langle p_{\rm abs}\rangle$. For increasing frequency, the peaks in the B/n_0-profiles of the $\langle\varepsilon\rangle$ and $\langle p_{\rm abs}\rangle$ are shifted to the right. For each value of the field frequency, $\langle\varepsilon\rangle$ and $\langle p_{\rm abs}\rangle$ initially increase with B/n_0, reaching a peak, and then they start to decrease with B/n_0. This is a typical resonant behavior although additional peaks observed for collisionless motion in the limit of higher B/n_0 are not observed. However, the position of the central and dominant peak in the B/n_0-profiles of $\langle p_{\rm abs}\rangle$ for molecular oxygen agree very well with the corresponding peak observed for collisionless motion of a single electron shown in figure 2. This is a clear sign that resonant absorption of the energy for collisionless motion carries over to the situation where collisions control the swarm behavior.

Temporal variations of the longitudinal W_E drift velocity over a range of magnetic fields for electrons in molecular oxygen are shown in figure 12. The electric field amplitude and frequency are set to 200 Td and 500 MHz, respectively. When a dc magnetic field is applied we observe a reduction in modulation amplitude of W_E and the modification of the phase shift between W_E and the electric field. It is interesting to note that for B/n_0 of 750 Hx there is no phase difference between W_E and electric field. However, the maximal absorption of energy occurs for lower B/n_0, around 550 Hx, as shown in figure 11. This follows from the fact that the modulation amplitude of

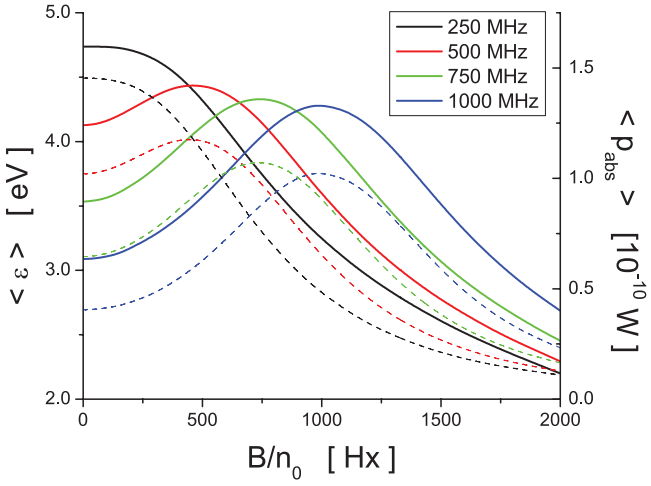

Figure 11. Variation of the cycle-averaged mean energy (full lines) and cycle-averaged power (dash lines) with B/n_0 for different field frequencies f. Calculations are performed for molecular oxygen. The amplitude of electric field is 200 Td.

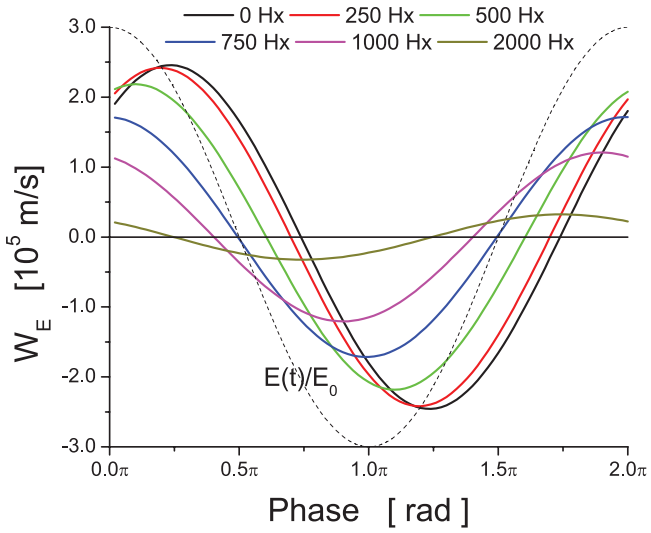

Figure 12. Temporal variations of the longitudinal drift velocity components for a range of magnetic field strengths. Calculations are performed molecular oxygen ($E/n_0 = 200$ Td, $f = 500$ MHz).

W_E is significantly decreased for B/n_0 of 750 Hx and illustrates how the interplay between modulation amplitude of the longitudinal drift velocity and its phase shift with respect to the electric field directly influences the power absorption.

3.5. Electrons in time-varying rf electric and magnetic fields in the presence of collisions

Certainly the most complex situation is the behavior of electrons in rf electric and magnetic fields in the presence of collisions. In figures 13 and 14 we show the variation of the cycle-averaged mean energy and cycle-averaged power as a function of the magnetic field amplitude for Reid's inelastic ramp model and molecular oxygen, respectively. Electric and magnetic fields are in the crossed orientation and $\pi/2$ out of phase. The most prominent property in the B_0/n_0-profiles of $\langle\varepsilon\rangle$ and $\langle p_{\rm abs}\rangle$ is the presence of additional periodic

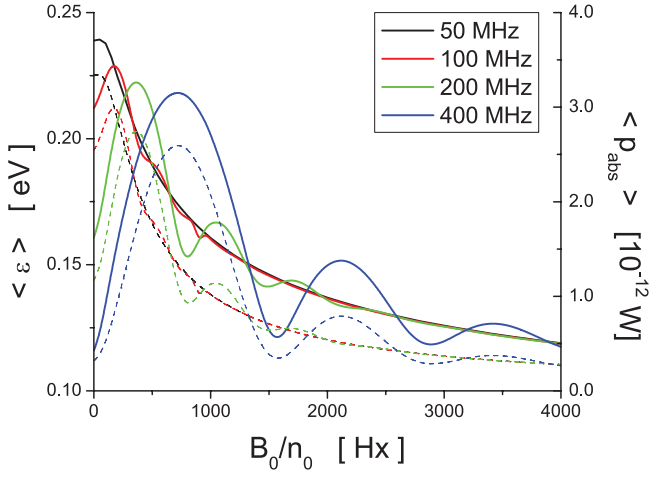

Figure 13. Variation of the cycle-averaged mean energy (full line) and power (dash line) with B_0/n_0 for different field frequencies. Calculations are performed for Reid's inelastic ramp model. The amplitude of electric field is 14.14 Td.

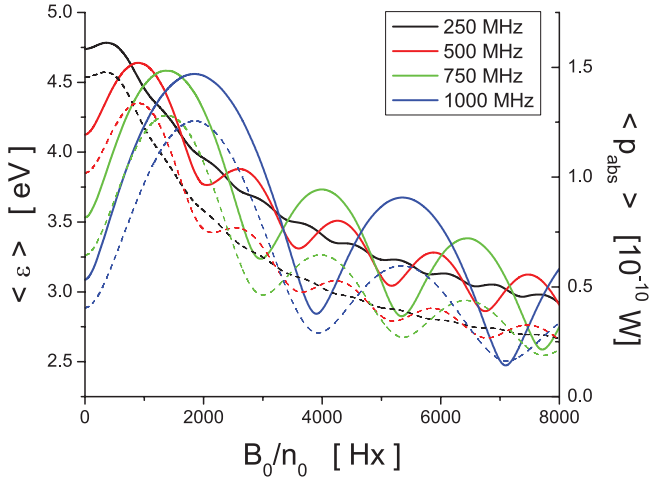

Figure 14. Variation of the cycle-averaged mean energy (full line) and power (dash line) with B_0/n_0 for different field frequencies. Calculations are performed for molecular oxygen. The amplitude of electric field is 200 Td.

structures. The positions of the extremes in $\langle\varepsilon\rangle$ are found to approximately correspond to those of $\langle p_{\rm abs}\rangle$. For increasing frequency, differences between positions of $\langle\varepsilon\rangle$ and $\langle p_{\rm abs}\rangle$ are slightly enhanced as the mean energy and drift velocity relax on different time-scales. For Reid's inelastic ramp model and frequencies lower than 50 MHz, $\langle\varepsilon\rangle$ and $\langle p_{\rm abs}\rangle$ are monotonically decreasing functions of the magnetic field amplitude. For higher frequencies, however, the resonant-type behavior is induced. In contrast to the situation where the electric field is radio-frequency and a magnetic field is static, we observe a multitude of peaks in the B_0/n_0-profiles of $\langle\varepsilon\rangle$ and $\langle p_{\rm abs}\rangle$. This is a clear signature of the resonant absorption of energy from the rf electric and magnetic fields. For increasing frequency, the periodic structures become more wider and extremes occur at higher values of B_0/n_0.

Temporal profiles of the longitudinal drift velocity component as a function of the magnetic field amplitude and

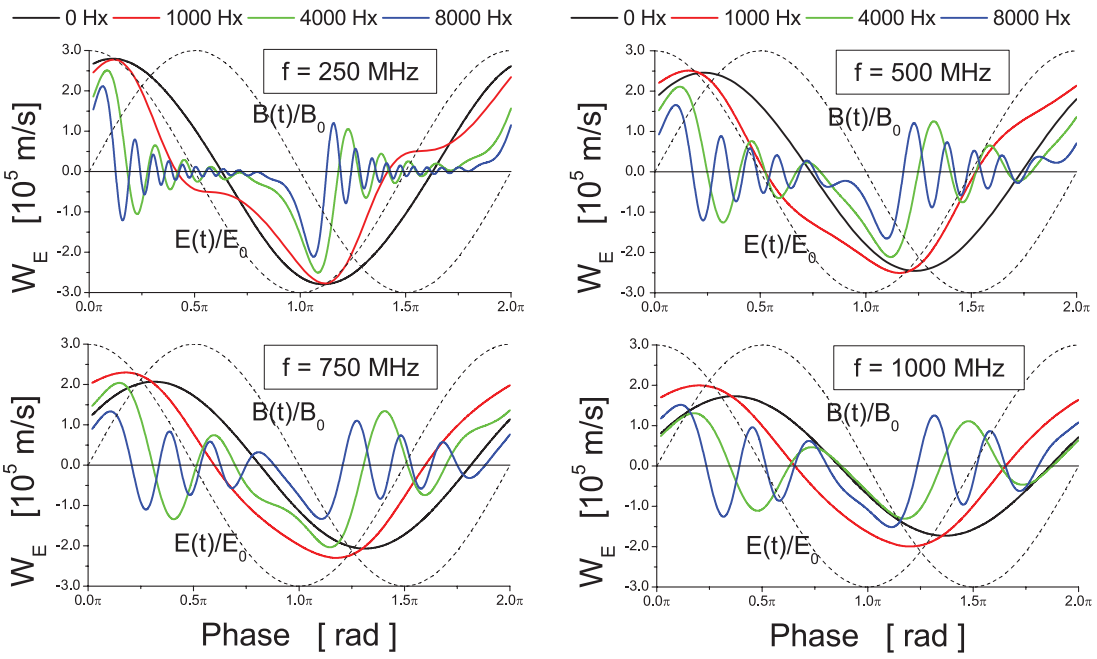

Figure 15. Temporal profiles of the longitudinal drift velocity component as a function of magnetic field amplitude and field frequencies. Calculations are performed for molecular oxygen. The amplitude of electric field is 200 Td.

frequency for electrons in molecular oxygen are shown in figure 15. For increasing B_0/n_0 the additional 'oscillatory'-type behavior in the W_E profiles is clearly evident for all frequencies considered in this work. For B_0/n_0 of 1000 Hx the modulation amplitude of W_E is increased as compared to the magnetic field free case while the phase shift with respect to the electric field is reduced. This favors the absorption of energy from the fields as shown in figure 14. Further increase of the magnetic field reduces the modulation amplitude and strong oscillations are induced. This is an alternating process which leads to the periodic structures observed in the absorbed power.

4. Discussion

The following question arises from the previous set of results: why do the periodic resonant structures exist for the absorbed power and mean energy in rf electric and magnetic fields? In low-frequency regime when all transport properties have enough time to relax, the physical mechanism of the magnetic cooling in dc electric and magnetic fields [15, 37, 66] is directly carried over to the rf fields. Under these conditions, the absorbed power is a monotonically decreasing function of the applied rf magnetic field amplitude (with the exception of the unusual behavior of mean energy for electrons in pure argon [39]). When the field frequency is increased, however, the phase shift between the drift velocity and electric field is enhanced. The number of electrons traveling against the field is significantly increased and the degree of their 'synchronization' with the electric field is reduced. In such a case, if the magnetic field is not too strong, then the action of the magnetic field perpendicular to the electric field (assuming that the electric and magnetic fields are crossed at an arbitrary angle) is to turn those electrons traveling against the electric field to travel with the electric field. In other words, the magnetic field

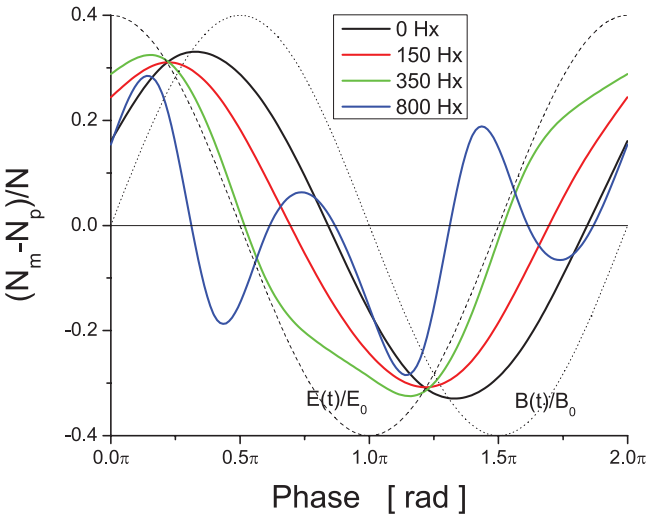

Figure 16. Temporal profiles of the difference between number of electrons traveling along (N_p) and against (N_m) the axis which is defined by the electric field. Calculations are performed for Reid's inelastic ramp model and N is total number of electrons in simulation. The amplitude and frequency of electric field are 14.14 Td and 200 MHz.

acts in such a manner to 'synchronize' electrons with the electric field. This physical picture is valid until reaching the first peak in the absorbed power versus amplitude of the applied rf magnetic field curve (see figures 13 and 14). Further increase of the applied rf magnetic field leads to a decrease of the absorbed power. Some aspects of these physical arguments are illustrated on figure 16 where the temporal profiles of the difference between number of electrons traveling with and against the electric field are calculated for several magnetic field amplitudes. Calculations are performed by our Monte Carlo code for Reid's inelastic ramp model. The amplitude and frequency are set to 14.14 Td and 200 MHz, respectively.

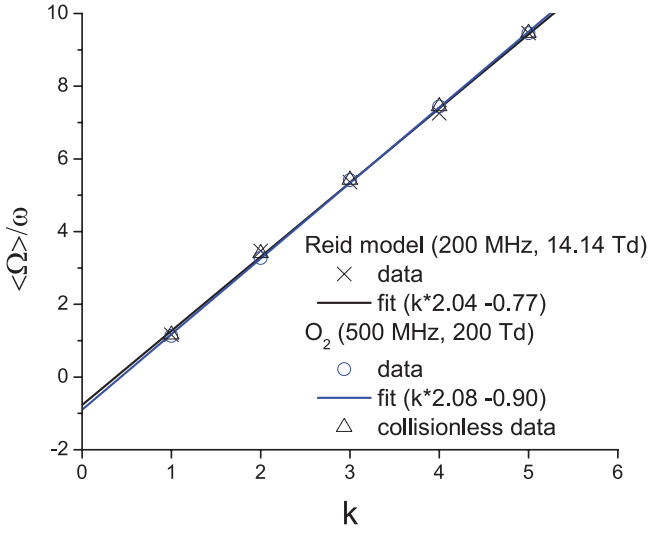

Figure 17. Positions of peaks in the absorbed power versus the ratio of mean cyclotron frequency to driving frequency.

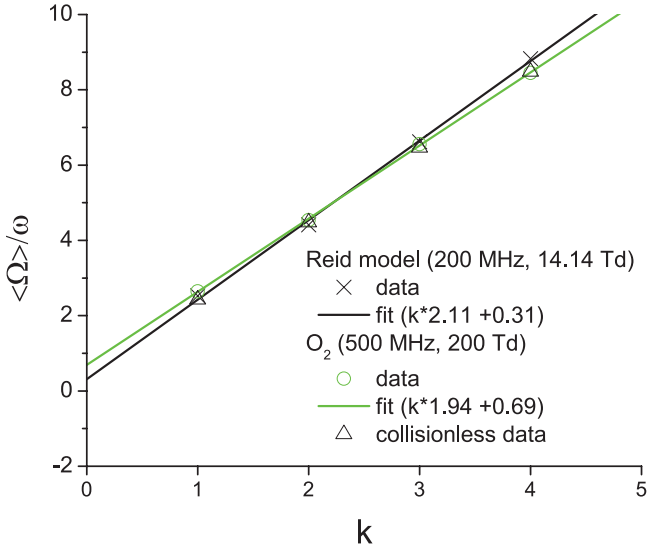

Figure 18. Positions of minima in the absorbed power versus the ratio of mean cyclotron frequency to driving frequency.

We see that the number of electrons traveling along the electric field is much greater for B_0/n_0 of 350 Hx than for the magnetic field free case. The phase shift between their oscillatory motion and oscillating rf electric field is much less comparing to the magnetic field free case and for cases where B_0/n_0 is set to 150 and 800 Hx.

In order to investigate the periodic nature of the resonant structures observed in figures 13 and 14, in figures 17 and 18 we show the positions of extremes in the absorbed power versus the amplitude of the applied rf magnetic field curve. We consider both the collision free case and situation when collisions control the swarm behavior for Reid's inelastic ramp model and molecular oxygen. In addition, we present the results of our linear fitting procedure for both the Reid ramp model and molecular oxygen. The cyclotron frequency is a sinusoidal function and thus we have decided to present its mean value which coincides with the amplitude of cyclotron frequency divided by $\pi/2$. We observe that the spacing between two successive peaks is constant and is approximately twice the field frequency. In other words, the slope of the fitting curves is approximately 2, as indicating in figures 17 and 18. We have found that the positions of the extremes are exclusively defined by the ratio between the mean cyclotron frequency $\langle\Omega\rangle$ and field frequency ω. As a consequence, the positions of the extremes are not dependent on the nature of the gaseous medium in which electrons drift and diffuse under the influence of rf electric and magnetic fields. Furthermore, we observe that numerical solutions for positions of the extremes in a collision free case agree very well with those obtained by solving Boltzmann's equation when collisions occur. This is a clear sign that even when collisions control the swarm behavior some amount of the energy is transferred to electrons via resonant absorption of the energy from the rf electric and magnetic fields.

5. Conclusion

In this paper we have analyzed, first, the collisionless motion of a single electron in spatially uniform rf electric and magnetic fields. The periodic feature in the absorbed power versus amplitude of the applied rf magnetic field curve has a typical resonant structure. When the power absorption peaks, the longitudinal and transverse velocity components are not periodic, their amplitude continuously increases with time and their mean values are not zero. On the other hand, when the absorbed power is zero, both velocity components are perfectly periodic with constant amplitudes.

Second, using a multi term theory for solving the Boltzmann equation, we have investigated the power absorption of electrons when collisions with neutral molecules occur. Numerical examples are given for electrons moving and diffusing under the action of rf electric and magnetic fields for Reid's inelastic ramp model and molecular oxygen. For magnetic field free case, the absorbed power shows the maximal property with frequency. In domain of rf fields, the absorbed power first increases with frequency, reaching a peak, and then it starts to rapidly decrease in the limit of higher frequencies. When a dc magnetic field is applied, the absorbed power first increases with increasing magnetic field, reaching a peak and then a rapid decrease follows. The maximum absorption of power occurs at magnetic field strengths for which simultaneously the phase shift between the longitudinal drift velocity and electric field is minimal and amplitude of drift velocity component is maximal. The position of the dominant peak on the absorbed power versus magnetic field strength curve coincides with the position of the same peak observed for collisionless motion of a single electron. This is a clear sign that the resonant absorption of energy takes place in both collisionless and collision-dominated regimes for electron swarms in rf electric and dc magnetic fields.

When both electric and magnetic fields are radio-frequency, the periodic structures in the absorbed power versus magnetic field amplitude strength curve are much more complex. We have observed a multitude of peaks in the B_0/n_0-profiles of the absorbed power and mean energy. Using numerical solutions for collisionless motion of a single electron and multi term

solutions of Boltzmann's equation when collisions occur, we have investigated the synergism of temporal non-locality and resonances and the interplay between these two effects. Perhaps the most striking phenomenon is the independence of the position of the extremes with respect to the gas in which electrons are drifting and diffusing.

In the past most plasma modeling has been carried out on the basis of swarm data for dc fields without any effect of magnetic field. We have tried to show here that the more elaborate representation of swarm transport theory would yield a far richer and more accurate description of heating of electrons in the complex case of combined electric and magnetic fields and their gradients.

There are few possible directions of future work arising from the results presented in this paper. The theory and mathematical machinery briefly presented in this paper, are valid for electric and magnetic fields crossed at arbitrary phases and angles. Therefore, the first logical extension of the current work would be to consider the effects of varying phases and angles between the fields on the power absorption. First steps have already been made towards this direction [34, 67]. Second, the theory and the associated code might be further extended to consider resonances induced by spatial non-locality as considered for electric field only in [54]. The ultimative goal would be to adapt the present theory in a form suitable for practical application to magnetized plasmas. This requires incorporation of the space charge effects through a multi term solution of Boltzmann's equation for both the electron and ion species in the discharge. It would be challenging and instructive to use this plasma-swarm nexus to explore the anomalous skin effect, negative absorption of power and complex electrodynamics of electrons in inductively coupled plasmas.

Acknowledgments

SD, DB and ZLjP acknowledge support from MPNTRRS Projects OI171037 and III41011. RDW is supported by the Australian Research Council.

References

[1] Petrović Z Lj, Šuvakov M, Nikitović Ž, Dujko S, Šašić O, Jovanović J, Malović G and Stojanović V 2007 *Plasma Sources Sci. Technol.* **16** S1
[2] Petrović Z Lj, Dujko S, Marić D, Malović G, Nikitović Ž, Šašić O, Jovanović J, Stojanović V and Radmilović-Radjenović M 2009 *J. Phys. D: Appl. Phys.* **31** 194002
[3] Shon C H and Lee J K 2002 *Appl. Surf. Sci.* **192** 258
[4] Shidoji E, Ohtake H, Nakano N and Makabe M 1999 *Japan. J. Appl. Phys.* **38** 2131
[5] Keidar M, Zhuang T, Shashurin A, Teel G, Chiu D, Lukas J, Haque S and Brieda L 2015 *Plasma Phys. Control. Fusion* **57** 014005
[6] Ahedo E 2011 *Plasma Phys. Control. Fusion* **53** 124037
[7] Makabe T and Petrović Z Lj 2015 *Plasma Electronics* 2nd edn (New York: CRC)
[8] Lieberman M A and Lichtenberg A J 2005 *Principles of Plasma Discharges and Materials Processing* 2n edn (New York: Wiley)
[9] Blum W and Rolandi L 1993 *Particle Detection with Drift Chambers* (Berlin: Springer)
[10] Bošnjaković D, Petrović Z Lj, White R D and Dujko S 2014 *J. Phys. D: Appl. Phys.* **47** 435203
[11] Petrović Z Lj, Raspopović Z M, Dujko S and Makabe T 2002 *Appl. Surf. Sci.* **192** 1
[12] White R D, Ness K F, Robson R E and Li B 1999 *Phys. Rev.* E **60** 2231
[13] White R D, Ness K F and Robson R E 2002 *Appl. Surf. Sci.* **192** 26
[14] Dujko S, Raspopović Z M and Petrović Z Lj 2005 *J. Phys. D: Appl. Phys.* **38** 2952
[15] Dujko S, White R D, Ness K F, Petrović Z Lj and Robson R E 2006 *J. Phys. D: Appl. Phys.* **39** 4788
[16] Sankaran A and Kushner M J 2002 *J. Appl. Phys.* **92** 736
[17] Dujko S, White R D, Petrović Z Lj and Robson R E 2011 *Plasma Sources Sci. Technol.* **20** 024013
[18] Loffhagen D and Winkler R 1999 *IEEE Trans. Plasma Sci.* **27** 1262
[19] Winkler R, Maiorov V A and Sigeneger F 2000 *J. Appl. Phys.* **87** 2708
[20] Winkler R, Loffhagen D and Sigeneger F 2002 *Appl. Surf. Sci.* **192** 50
[21] White R D, Robson R E and Ness K F 1995 *Aust. J. Phys.* **48** 925
[22] Maeda K, Makabe T, Nakano N, Bzenić S and Petrović Z Lj 1997 *Phys. Rev.* E **55** 5901
[23] Bzenić S, Petrović Z Lj, Raspopović Z M and Makabe T 1999 *Japan. J. Appl. Phys.* **38** 6077
[24] Raspopović Z, Sakadžić S, Petrović Z Lj and Makabe T 2000 *J. Phys. D: Appl. Phys.* **33** 1298
[25] White R D, Dujko S, Ness K F, Robson R E, Raspopović Z and Petrović Z Lj 2008 *J. Phys. D: Appl. Phys.* **41** 025206
[26] Dujko S, Raspopović Z M, Petrović Z Lj and Makabe T 2003 *IEEE Trans. Plasma Sci.* **31** 711
[27] Kolev St, Hagelaar G J, Fubiani G and Boeuf J-P 2012 *Plasma Sources Sci. Technol.* **21** 025002
[28] Zhao Y J, Liu H, Yu D R, Hu P and Wu H 2014 *J. Phys. D: Appl. Phys.* **47** 045201
[29] Benyoucef D and Yousfi M 2014 *Plasma Sources Sci. Technol.* **23** 044007
[30] Kinder R L and Kushner M J 2001 *J. Appl. Phys.* **90** 3699
[31] Tadokoro M, Hirata H, Nakano N, Petrović Z Lj and Makabe T 1998 *Phys. Rev.* E **57** R43
[32] Vasenkov A V and Kushner M J 2003 *J. Appl. Phys.* **94** 5522
[33] White R D, Robson R E, Dujko S, Nicoletopoulos P and Li B 2009 *J. Phys. D: Appl. Phys.* **42** 194001
[34] Dujko S 2009 *PhD Thesis* James Cook University, Australia
[35] Dujko S and White R D 2008 *J. Phys: Conf. Ser.* **133** 012005
[36] Dujko S, White R D, Petrović Z Lj and Robson R E 2010 *Phys. Rev.* E **81** 046403
[37] Ness K F 1994 *J. Phys. D: Appl. Phys.* **27** 1848
[38] Raspopović Z M, Sakažić S, Bzenić S and Petrović Z Lj 1999 *IEEE Trans. Plasma. Sci.* **27** 1241
[39] Ness K F and Makabe T 2000 *Phys. Rev.* E **62** 4083
[40] Vahedi V, Lieberman M A, DiPeso G, Rognlien T D and Hewett D 1995 *J. Appl. Phys.* **78** 1446
[41] Tuszewski M 1996 *Phys. Plasma* **4** 1922
[42] Kolobov V I and Economou D J 1997 *Plasma Sources Sci. Technol.* **6** R1
[43] Haas F A 2001 *Plasma Sources Sci. Technol.* **10** 440
[44] Lee H-C, Oh S J and Chin-Wook Chung C-W 2012 *Plasma Sources Sci. Technol.* **21** 035003
[45] Kushner M J, Collision W Z, Grapperhaus M J, Holland J P and Barnes M S 1996 *J. Appl. Phys.* **80** 1337
[46] Lloyd S, Shaw D M, Watanabe M and Collins G J 1999 *Japan. J. Appl. Phys.* **38** 4275

[47] Hollenstein Ch, Guittienne Ph and Howling A A 2013 *Plasma Sources Sci. Technol.* **22** 055021
[48] Scheubert P, Fantz U, Awakowicz P and Paulin H 2001 *J. Appl. Phys.* **90** 587
[49] Hash D B, Bose D, Rao M V V S, Cruden B A, Meyyappan M and Sharma S P 2001 *J. Appl. Phys.* **90** 2148
[50] Godyak V A, Piejak R B and Alexandrovich B M 1999 *J. Appl. Phys.* **85** 3081
[51] Cunge G, Crowley B, Vender D and Turner M M 2001 *J. Appl. Phys.* **89** 3580
[52] Vasenkov V A and Kushner M J 2002 *Phys. Rev.* E **66** 066411
[53] Minea T M and Bretagne J 2003 *Plasma Sources Sci. Technol.* **12** 97
[54] Nicoletopoulos P, Robson R E and White R D 2012 *Phys. Rev.* E **85** 046404
[55] Dormand J R and Prince P J 1980 *J. Comput. Appl. Math.* **6** 19
[56] Dujko S, White R D and Petrović Z Lj 2008 *J. Phys. D: Appl. Phys.* **41** 245205
[57] Dujko S, White R D, Raspopović and Petrović Z Lj 2012 *Nucl. Instrum. Methods Phys. Res.* B **279** 84
[58] Ness K F and Robson R E 1986 *Phys. Rev.* A **34** 2185
[59] Reid I 1979 *Aust. J. Phys.* **32** 231
[60] White R D, Brennan M J and Ness K F 1997 *J. Phys. D: Appl. Phys.* **30** 810
[61] White R D, Dujko S, Robson R E, Petrović Z Lj and McEachran R P 2010 *Plasma Sources Sci. Technol.* **19** 034001
[62] Itikawa Y, Ichimura A, Onda K, Sakimoto K, Takayanagi K, Hatano Y, Hayashi M, Nishimura H and Tsurubuchi S 1989 *J. Phys. Chem. Ref. Data* **18** 23
[63] Itikawa Y 2009 *J. Phys. Chem. Ref. Data* **38** 1
[64] White R D, Robson R E, Ness K F and Makabe T 2005 *J. Phys. D: Appl. Phys.* **38** 997
[65] Dujko S, White R D, Petrović Z Lj and Ebert U 2011 *Japan. J. Appl. Phys.* **50** 08JC01
[66] White R D, Ness K F and Robson R E 1999 *J. Phys. D: Appl. Phys.* **32** 1842
[67] Dujko S, Bošnjaković D, White R D and Petrović Z Lj 2015 in preparation